J. Geomag. Geoelectr., 27, 491-504, 1975

Running Waves and Standing Waves in Geomagnetic Depth Sounding

F.E.M. LILLEY

Research School of Earth Sciences,
Australian National University,
Canberra, A.C.T., Australia

(Received September 19, 1975; Revised November 18, 1975)

The process of electromagnetic induction in a layered half-space depends on the horizontal scale-length of the source field, whether it has the form of a running wave or a standing wave, and whether it consists of mixed modes. The theory as traditionally applied to geomagnetic depth sounding depends on approximating natural source-fields by single-mode running waves.

Magnetometer array data can be interpreted to show whether source fields are in fact running waves or standing waves. Phase maps of array data give wave-length estimates for running waves; amplitude maps of array data give field gradients (but usually not wave-length estimates) for standing waves. Commonly superpositions exist of both running waves and standing waves, indicating possible errors in traditional depth-sounding estimates which are based on the theory of a single-mode running wave.

Lack of source-field knowledge is a more serious disadvantage in traditional geomagnetic depth-sounding than it is in a newer method, which involves the ratio of vertical component to horizontal gradient measured from array data.

1. Introduction

This paper draws on the theory of electromagnetic induction in a horizontally layered half-space as developed by PRICE (1950, 1962), WHITHAM (1963), and SRIVASTAVA (1965). The notation and units of Price will be used. The basic results are as follows.

The half-space is considered composed of n layers, the jth layer having thickness h_j and electrical conductivity σ_j. The components of the electric field $\boldsymbol{E}$ and the magnetic field $\boldsymbol{H}$ are represented by (E_x, E_y) and (H_x, H_y, H_z) respectively, z being positive vertically down. The solution of the general induction problem is built up of elementary solutions of form

$$\boldsymbol{E}=\left(\frac{\partial P}{\partial y}, \frac{-\partial P}{\partial x}, 0\right)Ze^{i\omega t} \tag{1}$$

$$\boldsymbol{H}=\frac{i}{\omega}\left(\frac{\mathrm{d}Z}{\mathrm{d}z}\frac{\partial P}{\partial x},\ \frac{\mathrm{d}Z}{\mathrm{d}z}\frac{\partial P}{\partial y},\ \nu^2 ZP\right)\mathrm{e}^{i\omega t} \tag{2}$$

where i is $(-1)^{1/2}$, ω is angular frequency, and t is time. The function of depth $Z(z)$ satisfies

$$\frac{\mathrm{d}^2 Z}{\mathrm{d}z^2}=\{\nu^2+4\pi i\omega\sigma(z)\}Z \tag{3}$$

where ν is a constant and $\sigma(z)$ is the vertical distribution of electrical conductivity. The function of horizontal position $P(x, y)$ satisfies

$$\frac{\partial^2 P}{\partial x^2}+\frac{\partial^2 P}{\partial y^2}+\nu^2 P=0\,. \tag{4}$$

The surface impedance for n layers, (the lowest one extending to infinity), is given by

$$\frac{E_x}{H_y}=\frac{i\omega}{\theta_1 G_1(0)} \tag{5}$$

where

$$\frac{1}{G_1(0)}=\coth\left\{\theta_1 h_1+\coth^{-1}\left[\frac{\theta_1}{\theta_2}\coth\left[\theta_2 h_2+\coth^{-1}\left(\frac{\theta_2}{\theta_3}\coth\left(\theta_3 h_3+\cdots+\coth^{-1}\frac{\theta_{n-1}}{\theta_n}\right)\right)\right]\right]\right\},$$

and $\theta_j^2=\nu^2+4\pi i\omega\sigma_j$, $j=1, 2, \ldots, n$. (The $G_1(0)$ is SCHMUCKER's (1970) notation. SRIVASTAVA (1965) uses Z for E_x/H_y, but this is not adopted here to avoid confusion with the Z of Eq. (3)).

Three other relationships which hold between the field components are:

(i)
$$\frac{E_x}{H_y}=\frac{-i\omega}{\nu^2}\frac{1}{P}\frac{\partial P}{\partial x}\frac{H_z}{H_z}$$

so that

$$\frac{H_z}{H_x}=\frac{-\nu^2}{\theta_1 G_1(0)}\frac{P}{\partial P/\partial x} \tag{6}$$

(ii) (from SCHMUCKER, 1970)

$$\frac{H_z}{\partial H_x/\partial x+\partial H_y/\partial y}=\frac{1}{\theta_1 G_1(0)} \tag{7}$$

and

(iii)
$$\frac{\partial H_x/\partial x+\partial H_y/\partial y}{H_x+H_y}=\frac{-\nu^2 P}{\partial P/\partial x+\partial P/\partial y}\,. \tag{8}$$

Note that these relationships are for single values of ν, which might be regarded as individual modes of the source field, (the reciprocal of a ν value

giving a length scale, $\lambda=2\pi/\nu$). This is dictated by Eq. (4) which has solutions for P of form $\sin \nu x$, $\cos \nu x$, $e^{i\nu x}$, and $\sin(\nu_x x+\nu_y y)$ where $\nu_x^2+\nu_y^2=\nu^2$; but not of form $(\sin \nu_1 x+\sin \nu_2 x)$, $(\sin \nu_1 x+\cos \nu_2 y)$, etc. The solution $\sin(\nu_x x+\nu_y y)$ may appear to be a mixed mode but can be seen as a single mode upon rotation of the horizontal axes.

An alternative viewpoint to that taken in this paper is that the (only) single mode is of form $e^{i\nu x}$, so that $\cos \nu x$ and $\sin \nu x$ are each regarded as mixed modes, and a standing wave is seen as the combination of two different running waves, progressing in opposite directions. For the purposes of this paper, however, the contrast of running waves with standing waves may be based upon different and distinct mechanisms causing the two phenomena. A magnetic disturbance of running-wave nature will be caused by an electric current pattern which moves relative to an observer; a disturbance of standing-wave nature will be caused by an electric current pattern which stays stationary relative to an observer but which changes in strength with time.

2. Running Waves and Standing Waves

The theory thus far has been concerned with an elementary solution of the induction problem. The function $P(x, y)$ entering Eqs. (1) and (2) has not been restricted beyond requiring it to satisfy Eq. (4). It is now appropriate to consider different elementary P functions appropriate to the cases of running waves and standing waves in a source field.

2.1 Running waves

Take P to be of form

$$P(x)=e^{i\nu x} \tag{9}$$

where ν is pure real. Then it is easy to see that the field components vary with horizontal distance as does a running wave. For example, $\boldsymbol{E}$ from Eq. (1) becomes

$$\boldsymbol{E}=-i\nu Z e^{i(\nu x+\omega t)}\hat{y}\,. \tag{10}$$

Denoting the real and imaginary parts of a quantity X by $[X]_R$ and $[X]_I$ respectively, the real part of Eq. (10) becomes

$$[\boldsymbol{E}]_R=\nu\{[Z]_R \sin(\nu x+\omega t)+[Z]_I \cos(\nu x+\omega t)\}\hat{y}$$

with x and t dependence typical of a running wave.

For P of form (9),

$$\frac{1}{P}\frac{dP}{dx}=i\nu$$

so that Eq. (6) becomes

$$\frac{H_z}{H_x} = \frac{i\nu}{\theta_1 G_1(0)} . \tag{11}$$

This equation thus gives an expression for $\theta_1 G_1(0)$ in terms of the complex ratio H_z/H_x, and ν. Equation (11) has been the basis of what might be termed traditional geomagnetic depth sounding, as developed for example by PRICE (1962), WHITHAM (1963), CANER *et al.* (1967), COCHRANE and HYNDMAN (1970), and CANER (1971). Often the modulus of both sides of Eq. (11) is taken, thus losing the i factor and its significance, which is that there has been differentiation with respect to x of an assumed spatial dependence $e^{i\nu x}$.

Note also, for P of form (9), that Eq. (8) becomes

$$\frac{\mathrm{d}H_z/\mathrm{d}x}{H_z} = i\nu \tag{12}$$

so that an equation giving an estimate of ν is obtained. The right-hand-side of

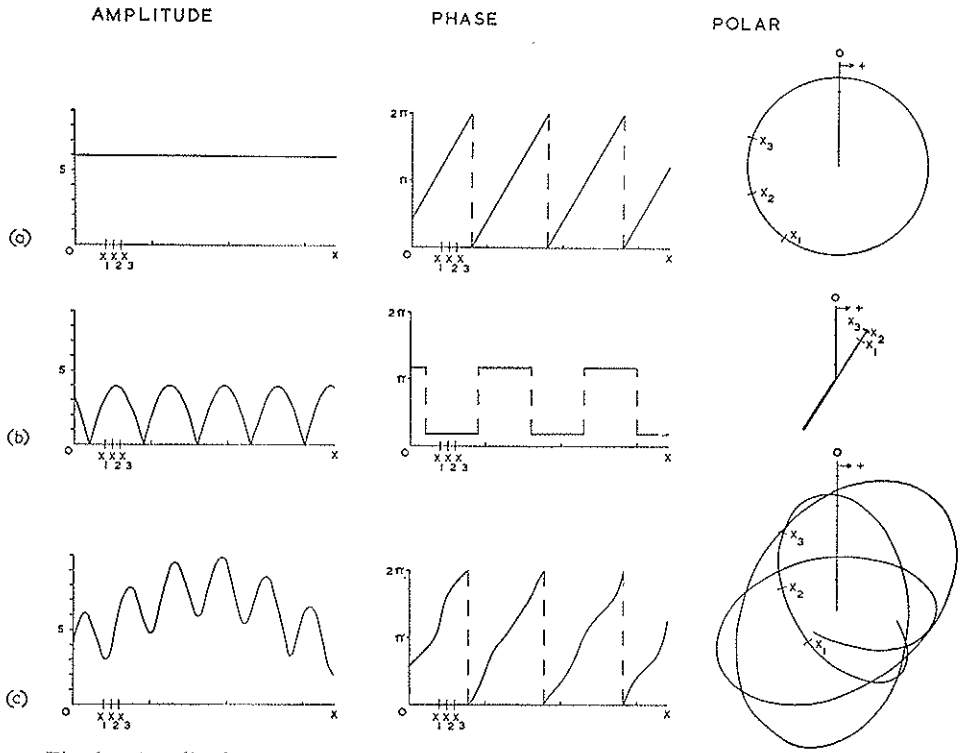

Fig. 1. Amplitude, phase, and polar characteristics of simple one-dimensional waves. (a) A running wave travelling in the $+x$ direction. (b) A standing wave. (c) The combination wave of (a) plus (b).

Eq. (12) is pure imaginary reflecting the fact that for a running wave observed for an indefinitely long time, the amplitude of H_x will be the same for all x, and that any variation with x (upon which $\mathrm{d}H_x/\mathrm{d}x$ may be calculated) will be found in the phase distribution. That is, if the characteristics of the wave are plotted as distributions of amplitude and phase against distance x, then the amplitude will be constant and the phase will vary. This principle will be referred to again in section 3.1 below, and is demonstrated in Fig. 1. Taking the modulus of both sides of Eq. (12) gives

$$\left|\frac{\mathrm{d}H_x/\mathrm{d}x}{H_x}\right| = \nu \tag{13}$$

but again at the risk of losing the significance of the i factor.

Note that the right-hand-sides of both Eqs. (12) and (13) are independent of x.

2.2 Standing waves

Taking P to be of form

$$P = \sin \nu x \quad \text{(with } \nu \text{ pure real)}, \tag{14}$$

standing waves are generated, for then $\boldsymbol{E}$ (for example) becomes

$$\boldsymbol{E} = -\nu Z \cos \nu x \, \mathrm{e}^{i\omega t}\hat{y}$$

the real part of which is

$$[\boldsymbol{E}]_R = -\nu\{[Z]_R \cos \omega t - [Z]_I \sin \omega t\} \cos \nu x \hat{y}$$

with x and t dependence typical of a standing wave.

For P of form (14),

$$\frac{1}{P}\frac{\mathrm{d}P}{\mathrm{d}x} = \nu \cot \nu x$$

so that Eq. (6) becomes

$$\frac{H_z}{H_x} = \frac{-\nu}{\theta_1 G_1(0)} \tan \nu x \,. \tag{15}$$

Equation (15) should be compared to Eq. (11) to see that no longer is an expression given for $\theta_1 G_1(0)$ independent of x: a factor $\tan \nu x$ is now present which will have a crucial effect, depending on where the nodes of the standing wave are relative to the point of H_z/H_x observation.

Note also that Eq. (8) becomes

$$\frac{\mathrm{d}H_x/\mathrm{d}x}{H_x} = -\nu \tan \nu x \tag{16}$$

again giving not a simple estimate of ν but one which may be greatly affected by the $\tan \nu x$ factor.

For this case it might be noted further that an expression involving a second derivative holds,

$$\frac{\mathrm{d}^2 H_x/\mathrm{d}x^2}{H_x} \equiv -\nu^2 \tag{17}$$

which does give an estimate of ν independent of any $\tan \nu x$ factor. For this to have practical application, however, a horizontal field would have to be known sufficiently accurately for its second derivative to be calculable.

2.3 Mixed-mode combinations

Mode combinations may occur in many ways, in one or both horizontal directions. Their separate contributions to the $\boldsymbol{E}$ field add together linearly, as do their separate contributions to the $\boldsymbol{H}$ field. The resultant expressions, like Eqs. (5), (6), (7) and (8) for E_x/H_y, H_z/H_x, etc., can then be computed, but will be complicated as these ratios for the individual modes do not add together linearly.

2.4 Implications for interpreting observed data

The use of Eq. (11) to interpret observed H_z/H_x data in terms of $\theta_1 G_1(0)$ is clearly valid only for a running-wave source-field of single mode. Any standing-wave component in the source-field will introduce error, by an undetermined but possibly large amount due to the $\tan \nu x$ factor on the right-hand-side of Eq. (15). Also, by comparing Eqs. (12) and (16) it can be seen that a local $(\mathrm{d}H_x/\mathrm{d}x)/H_x$ value can be relied upon as an estimate of the source-field wave-number ν only for a running wave of single mode, when in fact the estimate will be based upon phase data rather than amplitude data.

The magnetotelluric and array-gradient Eqs. (5) and (7), appear unaffected by whether the source field is of running-wave or standing-wave nature, (though for a standing-wave case, the relevant field components will become vanishingly small near the "nodes" of the standing wave). In these equations ν does not enter in the primary explicit manner with which it appears in the Eqs. (6) and (8); it does however enter in a secondary manner in the estimation of the θ_j values.

3. Information from Magnetometer Array Data

Magnetometer arrays, in which tens of instruments simultaneously record magnetic fluctuations over areas of order 10^5 km^2, may be expected to offer some information on the running or standing nature of the source fields. Data recorded by typical arrays show field behaviour in two dimensions over the horizontal area of observation.

Before presentation in map form, time-series data from array stations are typically Fourier-transformed into the frequency domain, thus giving for each

station at a particular frequency a value of amplitude and a value of phase. Maps of array data then simply show contour lines drawn around these various amplitude and phase values. The effect of the Fourier-transforming is such that although the original magnetic fluctuation events may have been discrete and aperiodic, the amplitude and phase values contained on the array data maps refer to contributions to the magnetic fluctuation events which are simple endless harmonic signals, and which may thus be analysed using theory based on a time dependence of $e^{i\omega t}$.

3.1 Significance of amplitude and phase maps

A running wave in one dimension has amplitude and phase distributions with distance as shown in Fig. 1a. Thus on maps of array data as commonly presented, such a wave will exhibit a featureless amplitude pattern, and a phase pattern of constant gradient in the direction of travel. A standing wave, shown in Fig. 1b, has by contrast a distinctive amplitude pattern, and a featureless phase pattern (with changes of $\pm\pi$ at the amplitude nodes). These then are diagnostic characteristics if found on array data maps. Superimposed modes will show definite patterns in both amplitude and phase, as in Fig. 1c (obtained by combining the patterns of Fig. 1a and b). Departures from horizontal layering in geologic structure may confuse array patterns by adding anomalous contributions to them.

Figure 1 also shows polar plots for the examples of running, standing, and combined modes. Such polar plots are an alternative way of portraying geomagnetic depth-sounding data. The characteristic of a running wave on a polar plot is a circle, of a standing wave is a straight line, and of two modes superposed is a complicated figure of many different possible shapes: the polar plot in Fig. 1c is one example.

Most arrays will span only part of a wave length of the source field, so that actual data if plotted will show only small parts of the patterns of Fig. 1; perhaps only those segments in every diagram between say x_1 and x_2.

3.2 Examples from south-east Australia

Two sets of magnetometer array data maps will now be analysed for running wave and standing wave characteristics, and reconnaissance horizontal field-gradient values estimated. Such horizontal field-gradient values can be seen to enter both Eqs. (7) and (8), and for horizontal layering they may be some of the most useful data produced by an array study. For convenience the gradients will be estimated in a normalized form: that is, $(\partial X/\partial x)/X$ rather than $\partial X/\partial x$.

Both sets of maps are from the 1971 array study in south-east Australia, shown in Fig. 2. In discussing them the notation (X, Y, Z) will be used for the

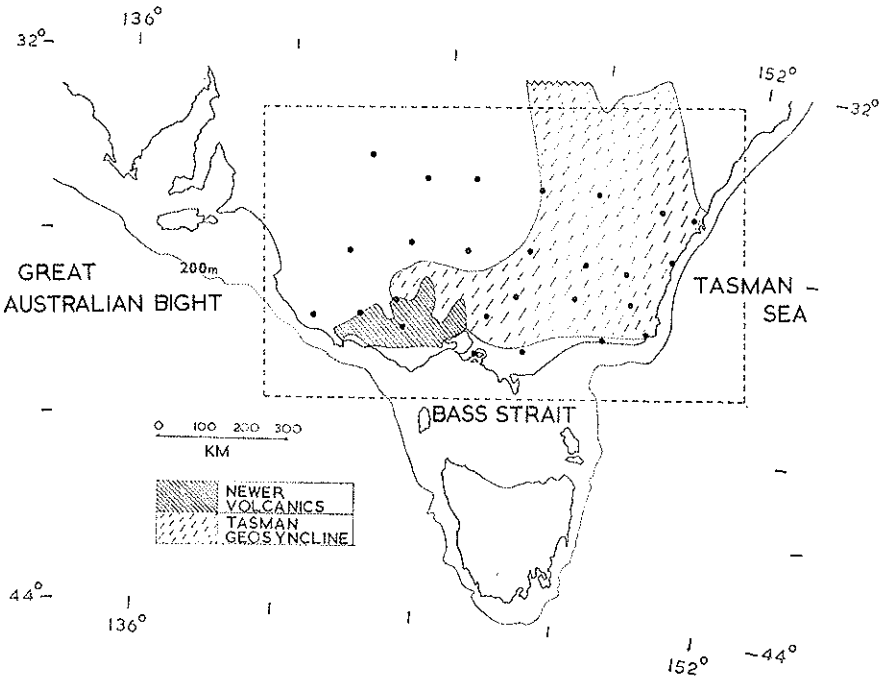

Fig. 2. Observation sites of the 1971 magnetometer array study in south-east Australia.

field components, equivalent to (H_x, H_y, H_z). The vertical field (Z) maps are included in the examples for completeness, but on their southern and eastern sides they are strongly affected by departures from horizontal layering in the electrical conductivity structure, (notably that of the coastline). Attention in this paper therefore concentrates on the horizontal field (X and Y) maps. These are little influenced by the coast effect and except at the central southern-most stations are thought to be fairly free from anomalous effects due to departures from horizontal layering in the geology.

Phases used in this paper are phase lags, in the sense that a more positive phase value corresponds to an event occurring at a later time. Estimates of $(\partial X/\partial x)/X$ are made in the following way. Two points are chosen which lie Δx apart in a north-south direction. The more northerly point has an X amplitude value of A, and an X phase (lag) value of α, and the more southerly point has corresponding values of B and β. Then an estimate of $(\partial X/\partial x)/X$ is obtained by computing

$$\frac{A\cos\alpha - B\cos\beta - i(A\sin\alpha - B\sin\beta)}{\Delta x(C\cos\gamma - iC\sin\gamma)}$$

where $C=(A+B)/2$ and $\gamma=(\alpha+\beta)/2$. Estimates of $(\partial Y/\partial y)/Y$ are made similarly.

For the special case of a running wave, $A=B=C$, and so

$$\frac{1}{X}\frac{\partial X}{\partial x}\approx -i\frac{\Delta\alpha}{\Delta x} \qquad \text{where} \qquad \Delta\alpha=(\alpha-\beta) \quad \text{radians.} \tag{18}$$

The right-hand-side of Eq. (18) is pure imaginary and based on phase data.

For the special case of a standing wave, $\alpha=\beta=\gamma$, and so

$$\frac{1}{X}\frac{\partial X}{\partial x}\approx\frac{A-B}{C\Delta x}\,. \tag{19}$$

The right-hand-side of Eq. (19) is real and based on amplitude data.

3.3 The ellipse of horizontal polarization

In interpreting array data maps it may be relevant to refer to the polarization ellipse of the horizontal field (LILLEY and BENNETT, 1972), and such ellipses are given for the examples discussed. They correspond in the present examples to representative X and Y amplitude and phase values for the central northern part of the array.

An important point in the present context is that non-zero ellipticity in the horizontal polarization ellipse necessarily indicates the presence of mixed modes. This can be seen from the fact that of the elementary P solutions given at the end of section 1, each by itself produces simple linear polarization.

3.4 Example 1

Figure 3 shows maps from BENNETT and LILLEY (1973) for the 12 hr component of three days of quiet variation in April 1971. The source field for such quiet daily variation is relatively well understood (MATSUSHITA, 1967). The X and Y maps show north-south gradients in amplitude, and east-west gradients in phase. Such a combination of patterns indicates a mixed-mode source-field, of standing-wave nature north-south and of running-wave nature east-west. This interpretation would be expected from the accepted model of the daily-variation source-field, which remains steady relative to the sun while the earth rotates beneath it.

The observed phase variation east-west across the array is 0.5 hr, (agreeing with the rate of passage of the sun). This gives a normalized east-west horizontal gradient which is pure imaginary,

$$\frac{1}{Y}\frac{\partial Y}{\partial y}=3.4i\times 10^{-4}\ \mathrm{km}^{-1}$$

indicating an east-west running wave of wavelength, using Eq. (12), of

$$\lambda=2\pi/\nu$$
$$=18500\ \mathrm{km}.$$

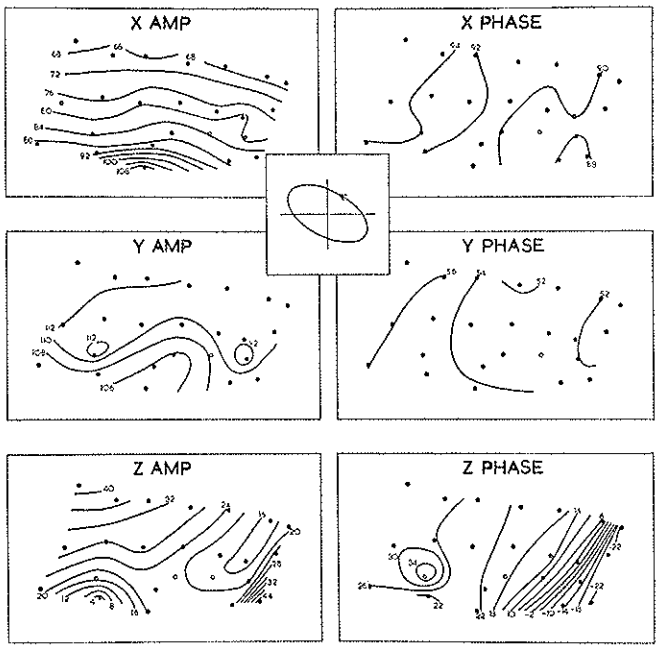

Fig. 3. Amplitude and phase maps from BENNETT and LILLEY (1973) for the 12 hr harmonic of three successive quiet days. Phase units are 1/10 hr, amplitude units are 1/10 nT.

From the north-south variation of amplitude a normalized field-gradient estimate is obtained which is pure real,

$$\frac{1}{X}\frac{\partial X}{\partial x} = -7.5\times 10^{-4}\,\mathrm{km}^{-1}\,.$$

Thus the knowledge of $(\partial X/\partial x)/X$ for the north-south standing wave does not give an estimate of its ν value. In principle, as pointed out in section 2.2, the second derivative $(\partial^2 X/\partial x^2)/X$ would give an estimate of ν^2 and hence ν. For most practical array data, however, it is expected that such second derivative estimates would be too uncertain to be useful.

3.5 Example 2

Figure 4 shows maps from LILLEY and BENNETT (1972) and BENNETT and LILLEY (1972), for the 85 min component of a substorm occurring on 19 March 1971. The horizontal variation data is first plotted resolved along geographic x (north) and y (east) axes, and then plotted again resolved along the x' (minor) and y' (major) axes of the horizontal polarization ellipse.

The X maps show east-west gradients in both amplitude and phase, indicating

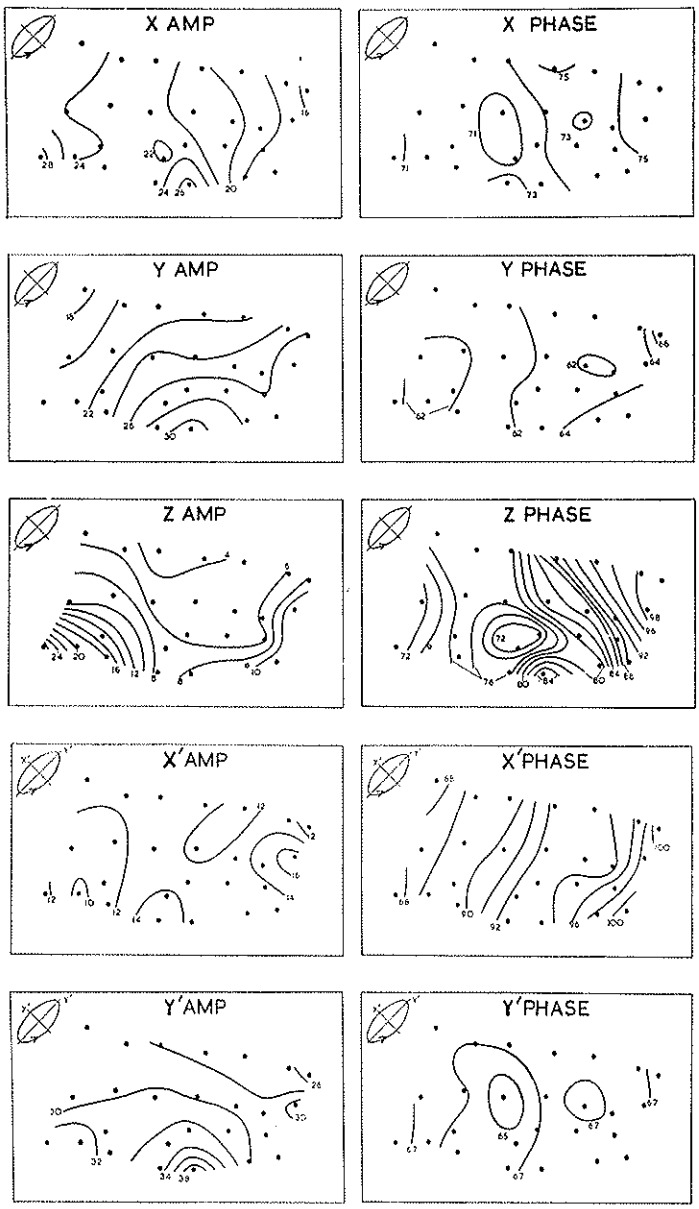

Fig. 4. Amplitude and phase maps from LILLEY and BENNETT (1972) and BENNETT and LILLEY (1972) for the 85 min period component of a substorm. Horizontal components are shown resolved both parallel to geographic co-ordinates (X and Y) and parallel to the axes of the horizontal polarization ellipse (X' and Y'). Phase units are minutes, and amplitude units are 21 nT-min.

a superposition of modes. The Y maps show a strong gradient in amplitude south-east-northwest, and a slight gradient in phase in the same direction. From such maps estimates of $(\partial X/\partial x)/X$ and $(\partial Y/\partial y)/Y$ can be made, (they will be complex), but these do not give estimates of ν.

The X' and Y' maps, however, appear to be more simple. The X' maps show only a gradient in phase, parallel to the X' direction. It is thus possible to estimate

$$\frac{1}{X'}\frac{\partial X'}{\partial x'} = 7.9i \times 10^{-4}\ \mathrm{km}^{-1}$$

the pure imaginary character of the right-hand-side indicating a running wave with $\nu = 7.9 \times 10^{-4}\ \mathrm{km}^{-1}$, and wave length of 7900 km.

The Y' maps show mainly a gradient in amplitude parallel to the Y' axis, giving the estimate

$$\frac{1}{Y'}\frac{\partial Y'}{\partial y'} = -4.4 \times 10^{-4}\ \mathrm{km}^{-1}\,.$$

Although the resolution shown of the X and Y fields into X' and Y' components was made initially for other purposes, the exercise appears to have simplified analysis of the source field. A physical interpretation is suggested in which the source field is caused mainly by a current flow parallel to the x' axis, with a strength which varies with time but with a spatial position which remains relatively steady somewhere off the diagram in the negative y' direction. Such a current flow will cause the standing-wave Y' pattern observed. The X' pattern is interpreted as being due to a current flow parallel to the y' axis, which sweeps in the $-x'$ direction (moving towards the south-east) at a rate appropriate to the X' phase.

Interpretations of array phase data in terms of current system motion were given by ROSTOKER *et al.* (1970) and BENNETT (1972). The present example demonstrates simplification by resolving the horizontal components parallel to the axes of their polarization ellipse.

From such analyses, magnetometer array data may hold much information on the ionospheric source-fields which cause induction in the earth. In a search for single-mode source-fields linear horizontal polarizations should be chosen, as elliptical polarizations indicate mixed modes.

4. Conclusions

The following points are made in conclusion.

4.1 The use of $H_z/(H_x^2+H_y^2)^{1/2}$ data for interpreting electrical conductivity profiles by way of Eq. (6) can be misleading if the source fields are not running waves.

4.2 Similarly the use of $(dH_x/dx)/H_x$ data (or its equivalent for a different component) for estimating ν by way of Eq. (13) can be misleading if the source fields are not running waves of limited ν range. For running waves, where application of the equation is correct, the calculation will be based on phase data, and amplitude data will be constant.

4.3 Some array maps, but not all, may allow estimates of source-field parameters. If ν estimates are needed for precise interpretation of geomagnetic depth-sounding data, the daily variation (S_q) source-field is attractive as being one of the best understood. However, even the S_q field is one of mixed modes, both of which may have to be taken into account to exploit it properly.

4.4 Do array data allow the separation of running modes from standing modes? Evidently in some cases this may be so, as shown by the examples discussed where the wave-motion (perhaps fortuitously) appeared to be standing in one direction and running at right angles to it. However amplitude and phase patterns occurring together cannot arbitrarily be split up, as shown by the combined-modes example of Fig. 1. If the complete amplitude and phase patterns are known then Fourier's theorem enables analysis of them; but if, as may be expected to be the case with array data, rather less than one wavelength of the patterns are known, prognosis for the general separation of modes is not optimistic.

4.5 Equation (5) (upon which traditional magnetotelluric interpretation is based) and Eq. (7) do not involve ν as strongly as does Eq. (6). Thus even when source-field parameters are not fully known, array maps over horizontally layered media should still permit the estimation of $\partial H_x/\partial x$ and $\partial H_y/\partial y$, and so an approximate application of Eq. (7) (SCHMUCKER, 1970; KUCKES, 1973).

4.6 Interpretations of magnetotelluric data by way of Eq. (5), and of array-gradient data by way of Eq. (7), are not affected by whether the source fields are of running-wave nature or of standing-wave nature.

I have benefitted greatly from correspondence and discussion on this subject with D.J. Bennett, P.A. Camfield, D.I. Gough, A.L. Hales, T.E. Holzer, A.F. Kuckes, S. Matsushita, R.L. Parker, U. Schmucker, and H.Y. Tammemagi. Mrs. M.N. Sloane assisted with Fig. 1.

REFERENCES

BENNETT, D.J., Geomagnetic depth sounding studies in south-eastern Australia, unpublished Ph. D. thesis, Australian National University, Canberra, 1972.

BENNETT, D.J. and F.E.M. LILLEY, Horizontal polarization in array studies of anomalous geomagnetic variations, *Nature Phys. Sci.*, **237**, 8-9, 1972.

BENNETT, D.J. and F.E.M. LILLEY, An array study of daily magnetic variations in southeast Australia, *J. Geomag. Geoelectr.*, **25**, 39-62, 1973.

CANER, B., Quantitative interpretation of geomagnetic depth-sounding in Western Canada, *J. Geophys. Res.*, **76**, 7202-7216, 1971.

CANER, B., W.H. CANNON, and C.E. LIVINGSTONE, Geomagnetic depth sounding and upper mantle structure in the Cordillera region of western North America, *J. Geophys. Res.*, **72**, 6335–6351, 1967.

COCHRANE, N.A. and R.D. HYNDMAN, A new analysis of geomagnetic depth-sounding data from western Canada, *Can. J. Earth Sci.*, 7, 1208–1218, 1970.

KUCKES, A.F., Relations between electrical conductivity of a mantle and fluctuating magnetic fields, *Geophys. J.R. astr. Soc.*, **32**, 119–131, 1973.

LILLEY, F.E.M. and D.J. BENNETT, An array experiment with magnetic variometers near the coasts of south-east Australia, *Geophys. J.R. astr. Soc.*, **29**, 49–64, 1972.

MATSUSHITA, S., Solar quiet and lunar daily variation fields, in *Physics of Geomagnetic Phenomena*, edited by S. Matsushita and W.H. Campbell, pp. 301–424, Academic Press Inc., New York, 1967.

PRICE, A.T., Electromagnetic induction in a semi-infinite conductor with a plane boundary, *Quart. J. Mech. App. Math.*, **3**, 385–410, 1950.

PRICE, A.T., The theory of the magnetotelluric method when the source field is considered, *J. Geophys. Res.*, **67**, 1907–1918, 1962.

ROSTOKER, G., C.W. ANDERSON, D.W. OLDENBURG, P.A. CAMFIELD, D.I. GOUGH, and H. PORATH, Development of a polar magnetic substorm current system, *J. Geophys. Res.*, **75**, 6318–6323, 1970.

SCHMUCKER, U., Anomalies of geomagnetic variations in the southwestern United States, *Bull. Scripps Inst. Oceanog.*, **13**, Univ. of California, 1970.

SRIVASTAVA, S.P., Method of interpretation of magnetotelluric data when source field is considered, *J. Geophys. Res.*, **70**, 945–954, 1965.

WHITHAM, K., An anomaly in geomagnetic variations at Mould Bay in the arctic archipelago of Canada, *Geophys. J.R. astr. Soc.*, **8**, 26–43, 1963.